Carrier dynamics of $In_xGa_{1-x}N$ quantum disks embedded in GaN nanocolumns

Mark J. Holmes,[1] Young S. Park,[1,a)] Xu Wang,[1] Christopher C. S. Chan,[1] Anas F. Jarjour,[1] Robert A. Taylor,[1,b)] Jamie H. Warner,[2] Jun Luo,[2] H. A. R. El-Ella,[3] and R. A. Oliver[3]

[1)] *Clarendon Laboratory, Department of Physics, University of Oxford, Parks Road, Oxford OX1 3PU, United Kingdom.*

[2)] *Department of Materials, University of Oxford, Parks Road, Oxford OX1 3PH, United Kingdom.*

[3)] *Department of Materials Science and Metallurgy, University of Cambridge, Pembroke Street, Cambridge CB2 3QZ, United Kingdom.*

Time-integrated and time-resolved microphotoluminescence studies have been performed on $In_xGa_{1-x}N$ quantum disks at the tips of GaN nanocolumns. The results are analysed in the context of current theories regarding an inhomogeneous strain distribution in the disk, which is theorised to generate lateral charge separation in the disks by strain induced band bending, an inhomogeneous polarization field distribution, and Fermi surface pinning. It is concluded that no lateral separation of carriers occurs in the quantum discs under investigation. Internal field screening by an increased carrier density in the QDisks at higher excitation densities is observed via a blue-shift of the emission, and a dynamically changing decay time. Other possible explanations for these effects are discussed and discounted. Cathodoluminescence studies have also been carried out on the nanocolumns to provide insight to the physical origin of the luminescence.

PACS numbers: 61.27.uj, 63.20.kk, 81.07.Vb

[a)] Also at: Center for Superfunctional Materials, Pohang University of Science and Technology, Pohang 790-784, Korea.

[b)] Electronic mail: r.taylor1@physics.ox.ac.uk

I. INTRODUCTION

III-Nitride semiconductor-based structures are enjoying success in optoelectronic device applications, due largely to the wide direct band gap exhibited by GaN, enabling efficient high energy emission[1,2]. The ability to incorporate either indium or aluminium, during growth, to form ternary/quaternary compounds enables the construction of crystals with a wide range of band gap energies and hence emission wavelengths[3]. When in the Wurtzite crystal structure (space group $P6_3mc$) these structures will be at the mercy of an inbuilt electric field that has components due to both a spontaneous polarisation and a strain induced piezoelectric field ($P6_3mc$ is a non-centrosymmetric group). In nanostructures the effect of these fields (which have a combined magnitude[4–7] of order MVcm^{-1}) is to redshift the energy spectrum, and increase the emission lifetime by the quantum confined Stark effect (QCSE).

It has been reported that III-Nitride nanocolumns may be a solution to this problem due to their larger surface/volume ratio and inherent strain relaxation[8,9], which can lead to a suppressed internal field[10]. However, any quantum well (QW) which is grown as part of a nanocolumn to form a quantum disk (QDisk) will indeed be under strain due to a lattice mismatch. Furthermore, the strain profile has been shown to be inhomogeneous in the plane of the well due to a relaxation process at the QDisk edges[11,12]. The inhomogeneity in strain can result in a lateral inhomogeneous distribution of charge carriers in the QDisk owing to band bending by deformation potentials and an inhomogeneous polarization field. In this communication we investigate, through experimental results, the distribution of charge in $In_xGa_{1-x}N$ ($x \sim 0.1$) QDisks grown on GaN nanocolumns. We begin by describing the sample structure (section II), and then present a calculation showing a strain distribution for a typical, low indium content, QDisk (section III). In sections IV and V we characterise the samples using cathodoluminescence (CL) and microphotoluminescence (μPL) spectroscopic techniques and comment on the implications for the distribution of carriers in the QDisks.

II. SAMPLE STRUCTURE AND PREPARATION

The GaN columns used in this investigation were grown under nitrogen rich conditions by RF-plasma assisted molecular beam epitaxy (PAMBE) on Si (111) substrates[13–15]. Two

growth regimes are apparent in the samples; a compact region resulting from the coalescence of low aspect ratio columns, and the nanocolumns themselves. The columns are typically $\sim 140\,\mathrm{nm}$ in diameter and about $2\,\mu$m to $4\,\mu$m in length, with a density of $\sim 1 \times 10^9\,\mathrm{cm}^{-2}$. 2.5 nm thick $\mathrm{In}_x\mathrm{Ga}_{1-x}\mathrm{N}$ quantum well layers with a nominal mole fraction of 0.1 were grown on top of the columns to form quantum disks (QDisks). These disks were then capped with $\sim 3\,\mathrm{nm}$ of GaN. The well thickness and indium mole fraction were estimated by interpolation of a high resolution x-ray diffraction pattern measured from an InGaN epilayer grown under the same conditions. The QDisks provide both a strong carrier confinement in the growth direction and a degree of lateral confinement due to the limited diameter of the columns/disks. The disks were grown at reduced temperature (700^oC as opposed to 900^oC for the nanocolumn growth), to facilitate the incorporation of indium.

The sample investigated during this study had a single QDisk grown on the columns. The average column diameter, measured at the widest point, was found to be 140 nm. Electron microscope images of the columns, and a histogram detailing the size distribution, can be found in figure 1.

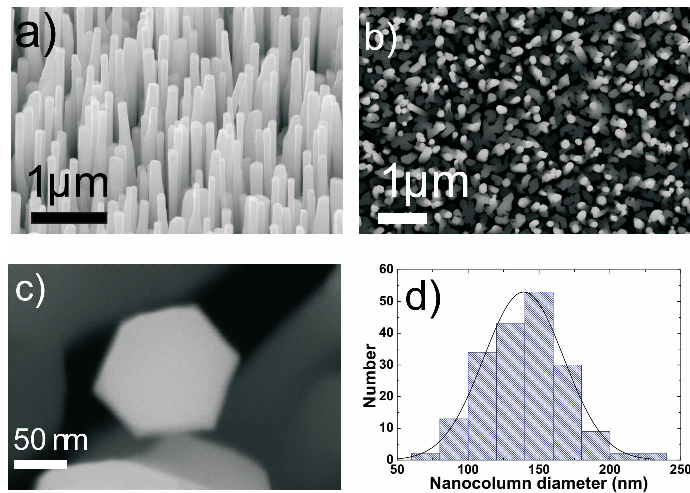

FIG. 1. Electron microscope images of the sample under investigation. a) SEM micrograph of the as-grown GaN nanocolumns. b) Plan view SEM micrograph showing the columns and compact regions. c) SEM micrograph showing the cross section of a single hexagonal GaN nanocolumn. d) Histogram detailing the size distribution of the nanocolumns.

In this communication we present results from a sample with a single QDisk only, although we note that we have measured similar results in other samples with 2 and 5 QDisk stacks.

III. STRAIN CALCULATIONS AND CARRIER DISTRIBUTION CONSIDERATIONS

The strain distribution for a 2.5 nm thick $In_{0.1}Ga_{0.9}N$ QDisk of diameter 140 nm in a GaN nanocolumn has been calculated using the next**nano**[3] device simulator. The xx component of the strain tensor ϵ and also the hydrostatic strain ($= \epsilon_{xx} + \epsilon_{yy} + \epsilon_{zz}$) in the xz plane (z is the growth direction) are presented through a cross section of the column/disk, along with a bright field TEM micrograph of a single column, in figure 2. The distribution of hydrostatic strain is found to resemble that observed in the TEM image, and the distribution of ϵ_{xx} calculated here (c) compares well with those published for similar structures[12], albeit with reduced magnitude owing to the lower indium content of the QDisk in this investigation. The QDisk is predominantly under compressive strain in the xy-plane and under tensile strain along the z (growth) axis. ϵ_{xx} varies by nearly 2 orders of magnitude from from $-1.1\,\%$ at the centre of the disk to an almost completely relaxed value of $-0.05\,\%$ at the edge. We note that the column is wider at the tip. This could be due to either a strain relaxation process which results in a deformation of the column tip, or an increase in lateral growth rate during the InGaN growth. During the simulation, however, the side walls of the nanocolumn/QDisk were kept at a constant diameter of 140 nm.

The inhomogeneity in strain distribution leads to a non uniform piezoelectric field across the diameter of the disk and also a bending of both the conduction and valence bands due to deformation. These two processes can result in a non-trivial band profile in the xy-plane and it has been suggested that this may result in lateral carrier separation within the QDisk[8,11,16]. The exact location of the confinement for electrons and holes depends on the geometry of the QDisk and surrounding material, as well as on the potential depth of the disk relative to the surrounding material. Fermi pinning can also play a role in creating accumulation or depletion layers at the surface[17,18]. These effects will be discussed further in section V.

IV. DETERMINATION OF THE NANOCOLUMN/QDISK LUMINESCENCE SPECTRUM

In figure 3 a) we present a cathodoluminescence (CL) emission spectrum of an ensemble of nanocolumns. The spectrum was acquired at 90 K with an accelerating voltage of 10 kV.

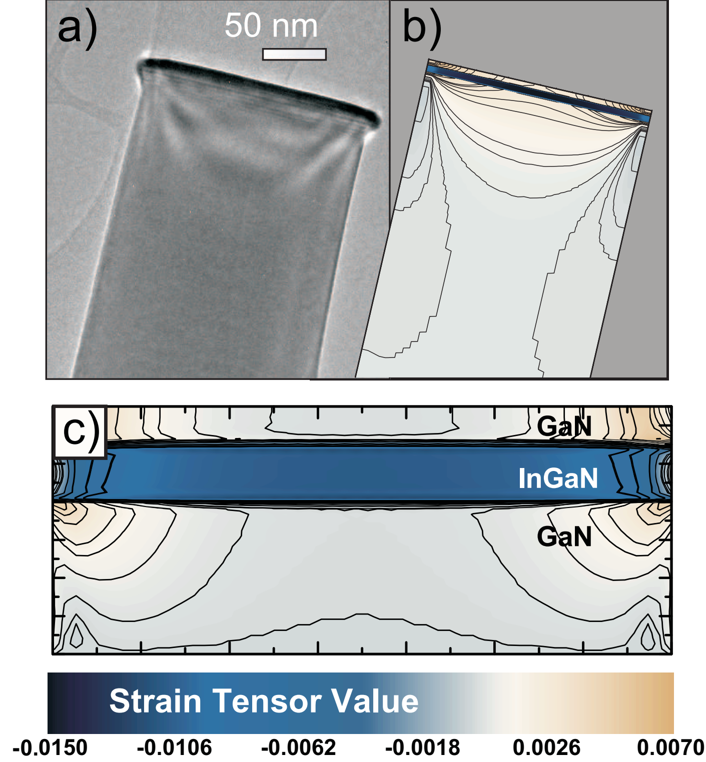

FIG. 2. a) A TEM image of the tip of a single GaN nanocolumn. b) A simulation of the distribution of hydrostatic strain in a cross section through the column. c) The strain distribution (ϵ_{xx}) in the region of the QDisk.

The luminescence was recorded by a MonoCL4 system with a 2400 lmm^{-1} diffraction grating. μPL spectra recorded at 4.2 K and 90 K are presented for comparison (see section V for details of the μ-PL setup).

Three main emissions are present in both the CL and PL spectra. The emission at $\sim$ 3.47 eV is attributed to the I2 emission from the GaN nanocolumn, and the broad emission in the region 3.40 eV - 3.44 eV is typically attributed to carrier recombination at basal stacking faults (BSFs); the I1 transition[9]. The emission at $\sim$ 3.34 eV is highly focus dependent and is attributed to the emission from the $In_xGa_{1-x}N$ QDisk at the tips of the columns.

The elevated temperature CL and μPL spectra show a much broader emission than the low temperature μPL spectra. This is most likely due to the increased thermal energy of the carriers injected/excited into the structures. The CL spectrum was recorded by scanning the electron beam across, and integrating the luminescence from, a 5.5 μm^2 area of the sample. The μPL spectra were recorded from an area of 0.8 μm^2 corresponding to the laser spot size.

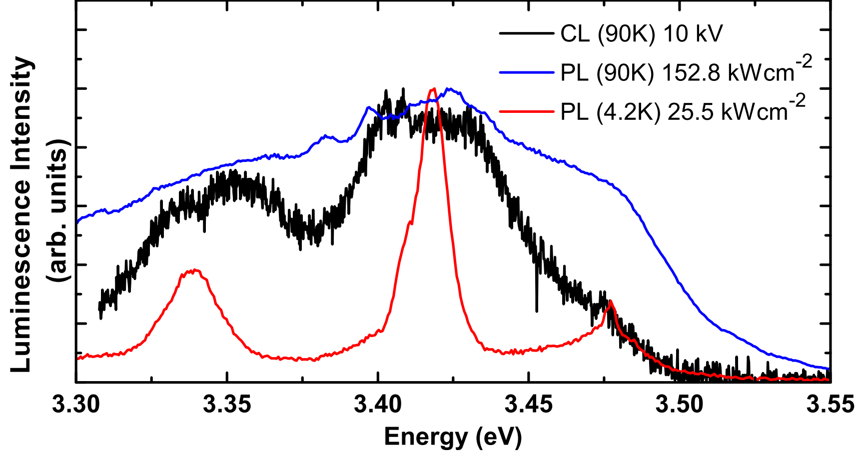

FIG. 3. CL emission spectrum from an ensemble of QDisk containing nanocolumns recorded at 90 K with an accelerating voltage of 10 kV (black). μPL spectra from the same sample recorded at 4.2 K (red) and 90 K (blue) are show for comparison.

The 90 K μPL spectra was recorded with a much increased excitation power, as the intensity of the emission is found to decrease for temperatures greater than 20 K, as shown in section V.

The spatial origin of the luminescence was verified by scanning the electron beam across the sample surface on a clump of felled nanocolumns. The results presented in figure 4 consist of 3 images showing the emission from the GaN (red), defect (blue) and QDisk (green) superimposed on a secondary electron SEM micrograph of the region under investigation. The accelerating voltage used during the acquisition of these images was 5 kV.

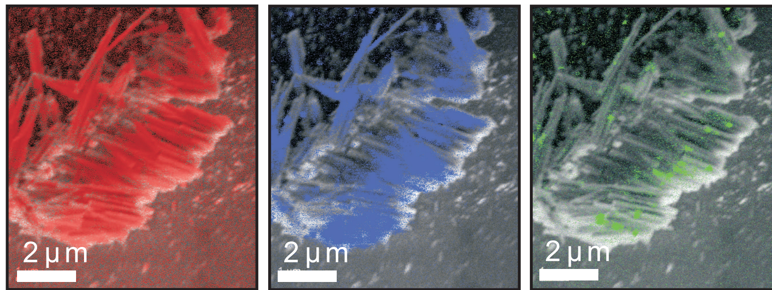

FIG. 4. The emission from the GaN (red), defect (blue) and QDisk (green) superimposed on a SEM micrograph of the felled nanocolumns. In contrast to the GaN and defect emission, the QDisk emission is highly spatially localised, and originates near the tips of the columns.

It is immediately apparent that both the GaN and defect emissions originate from the body of the columns, whereas the InGaN QDisk emission is more spatially localised, and comes from the region near the tips of the columns. It is also observed that the bases of the columns appear to be optically inactive, perhaps due to damage incurred during the felling process.

V. μ-PL EXPERIMENTS ON AS-GROWN COLUMNS

Time-integrated microphotoluminescence studies were performed on the nanocolumns using a frequency tripled Ti:Al_2O_3 laser at 266 nm (120 fs pulses at 80 MHz). The samples were mounted in a continuous flow helium cryostat (Janis ST-500) with an attached temperature controller (Lakeshore 331) such that the temperature could be measured and controlled accurately. The laser was focussed on the as grown-columns to a spot size of 0.8 μm^2 by a 36× reflecting objective (Ealing EA-25-0522-000), this spot size corresponding to simultaneous excitation of approximately 8 nanocolumns. PL was collected by the same objective and dispersed by a 1200 lmm^{-1} reflecting grating before being measured on a Peltier-cooled silicon charged coupled device (CCD). The spectrometer (Andor Technology Shamrock SR-303i) has a spectral resolution of $\sim$ 0.1nm. For time-resolved studies, the PL was directed through a 50 μm slit (giving a spectral resolution of $\sim$ 0.2 nm) to a photomultiplier tube (PMT) with a temporal resolution of 130 ps. A commercial time correlated single photon counting PC card (Becker & Hickl SPS630) was used to measure the emission lifetimes.

A. Temperature dependent time-resolved μ-PL studies and the subsequent implications for the carrier distribution in the QDisk

Typical time-resolved and time-integrated emission spectra at temperatures from 4 K to 70 K (excitation power density = 4.1 $kWcm^{-2}$) from a single QDisk in a nanocolumn (isolated spectrally) are presented in figure 5. The emission decay at 4.2 K in the figure 5 b) inset is observed to have a monoexponential profile with a lifetime of $\sim$ 7 ns. As the temperature is increased above 20 K the decay becomes non-exponential and the characteristic decay time (measured as the time taken for the intensity to reach 1/2 of its peak value) is found to decrease with increasing temperature. This coincides with the decrease in emission intensity

of the QDisk emission for temperatures greater than 20 K. This effect is most probably due to non-radiative decay routes opening up at higher temperatures. We note that there is no apparent blue shift (S-curve) of the emission with increasing temperature, indicating that there is not a large degree of carrier localisation due to indium content fluctuations in the disk. Indeed, low indium content QWs are usually observed to have lower indium content variation, and analysis of the peak indicates that the indium mole fraction, x, in this case is ~ 0.07. We therefore put an upper limit on the energy state variations due to indium fluctuations as half of the peak FWHM: ~ 4 meV. We do note, however, that fluctuations in the well width across the diameter of the disk may result in a deeper confinement (of order 50 meV) that we couldn't hope to observe in the temperature range probed here.

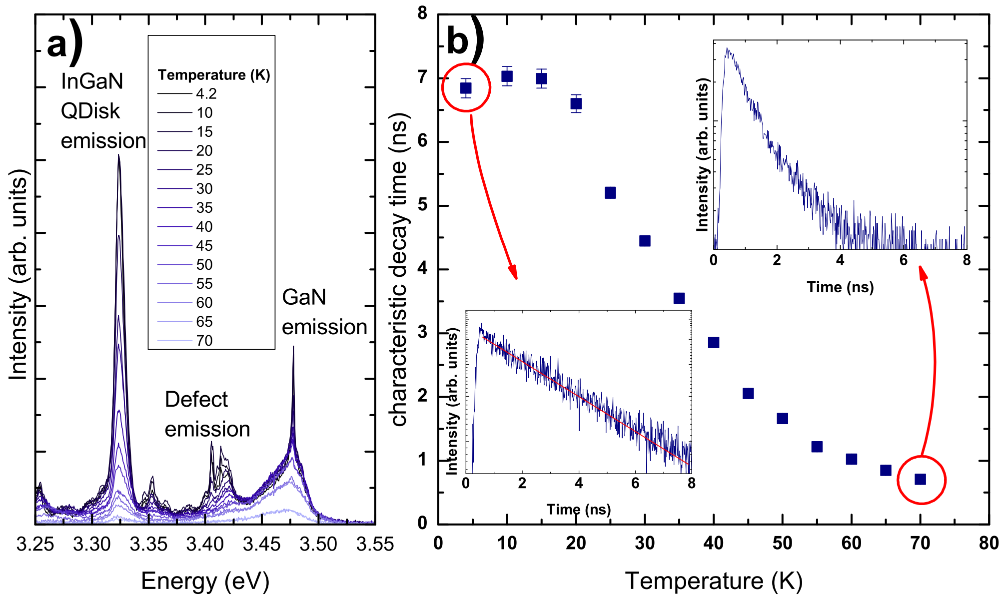

FIG. 5. a) Time-integrated spectra from the as-grown nanocolumns at temperatures from 4 K to 70 K. b) Time-resolved studies showing a sudden decrease in lifetime for temperatures $T > 20$ K.

As well as providing information on the uniformity of the indium content in the QDisk, this data provides an immediate insight on the nature of the carrier distribution in the QDisk. The low temperature emission occurs with a lifetime of 7 ns, which is comparable to the values of $1 - 10$ ns published by Graham *et al.*[19] and Thrush *et al.*[20] for planar InGaN QWs of thickness $2.5 - 2.7$ nm and mole fraction $0.05 - 0.12$. In this regard, the QDisks act somewhat like planar QWs, as any further, lateral, separation of electron and

hole wavefunctions induced by strain relaxation at the disk edge would most probably result in much longer lifetimes than those measured. Indeed, several studies have experimentally verified that in the InGaN/GaN system, allowing the carrier wavefunctions to be further separated along the c-axis by varying the QW thickness results in a drastic increase of the emission lifetime: Chichibu *et al.*[21] showed that for $In_{0.1}Ga_{0.9}N$ MQWs the emission lifetime increases by an order of magnitude as the well thickness is varied from 1.2 nm to 5 nm. Ryu *et al.*[22] similarly showed that $In_{0.15}Ga_{0.85}N$ MQWs exhibit an order of magnitude increase in lifetime as the QW thickness is increased from 1 nm to 4 nm. A more extreme case was demonstrated by Zhang *et al.*[23] during their investigations on $In_{0.19}Ga_{0.81}N$ MQWs, when they measured a lifetime increase from 5.8 ns to 454 ns as the QW thickness was increased from 2.2 nm to 4.4 nm. In these referenced studies on planar QWs, there is still the possibility that the carriers are indeed somewhat laterally separated by a few nanometers due to individual confinement of electrons and holes at spatially distinct indium fluctuations[24,25]. The experimental evidence presented here, however, leads us to believe that the transition we observe is not due to the recombination of carriers which are further laterally separated due to the inhomogeneous strain distribution in the disk; a separation which, in the most extreme case, would be ~ 70 nm.

Böcklin *et al.*[16] calculated that for a (relatively high indium content) $In_{0.4}Ga_{0.6}N$/GaN QDisk system, the electrons may be confined at the periphery of the disk, and the holes at the disk centre. This is in contrast to the situation in GaN/AlGaN QDisk systems where, according to the calculations of Riviera *et al.*[11] it is the electrons that are to be found at the centre of the disk, and the holes at the edges. It should also be noted that the effects of Fermi level pinning at the free surface of the disk have been ignored in models of the two cases outlined above. The pinning potential ϕ can be of order 300 meV for $In_{0.1}Ga_{0.9}N$[18] and will result in a surface depletion layer. The size of ϕ is of the same order of the electron confinement at the QDisk edge calculated by Böcklin *et al.*[16]. It follows that it is quite plausible that, in the special case of low indium content InGaN QDisks, the three effects in the conduction band (deformation leading to confinement at the edge, and both polarization fields and Fermi pinning which lead to confinement at the disk centre) can sum to reveal a conduction band that doesn't strongly confine electrons in any one lateral position in the QDisk. Holes, on the other hand, may still be strongly localised, as the deformation of the valence band due to the inhomogeneous strain distribution is not as severe. This situation

could lead to a reasonable wavefunction overlap and result in decay lifetimes not to dissimilar to those from planar QWs.

B. Low temperature μ-photoluminescence studies: The quantum confined Stark effect

PL spectra from a different nanocolumn at 4 K as a function of excitation power density are presented in figure 6a. The QDisk emission is observed near 3.325 eV at an excitation power of 3.82 $kWcm^{-2}$. With increasing excitation power the QDisk emission shifts to higher energy, before saturating at $\sim$ 3.340 eV. The emission energy is plotted as a function of excitation power density in the figure inset. The integrated peak intensities of the QDisk emission and GaN emission are presented as a function of excitation power in figure 6b. The excitonic emission from the GaN is measured to increase almost linearly whereas the QDisk emission increases as the square of the excitation power. The quadratic nature of this increase indicates that the recombination in the QDisk is mainly due to free carriers.[26]

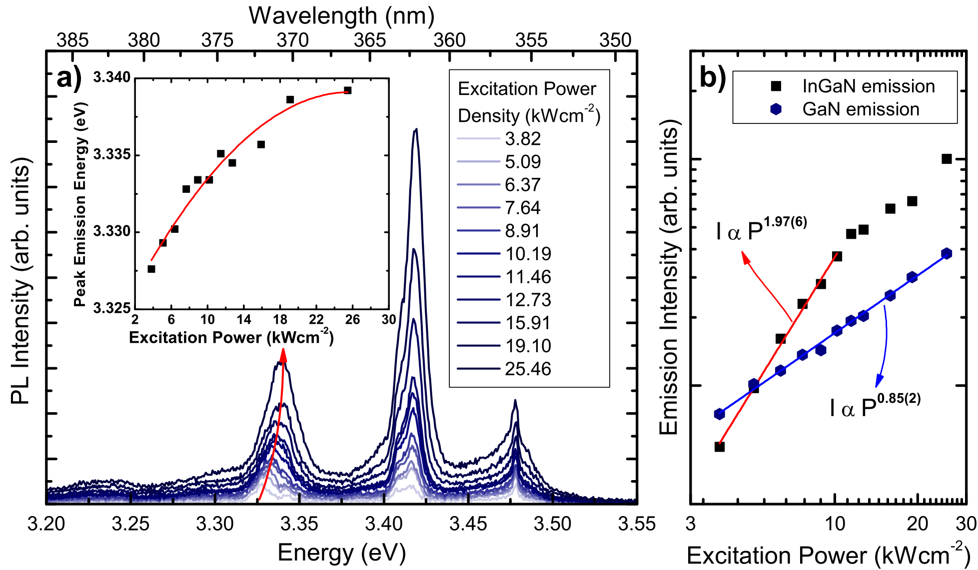

FIG. 6. a) InGaN QDisk emission as a function of excitation power. The inset shows the QDisk emission peak position with increasing excitation. The fit to the curve is quadratic, and has been used to estimate the indium mole fraction. b) A log-log plot of QDisk and GaN emission intensities.

Time-resolved μ-PL data is presented in figure 7. The low excitation power decay in

figure 7a is the characteristic mono-exponential decay from the QDisk[27]. As the emission is broader at higher excitation power, it is possible to measure the time resolved characteristics of the emission as a function of energy. Two such decays are presented in figure 7b. The decay from the high energy side of the emission is nonexponential, and has an initial rapid decay of 390 ps, before dynamically reverting to a longer decay time. The lower energy side of the emission shows a slightly delayed 3.5 ns monoexponential decay.

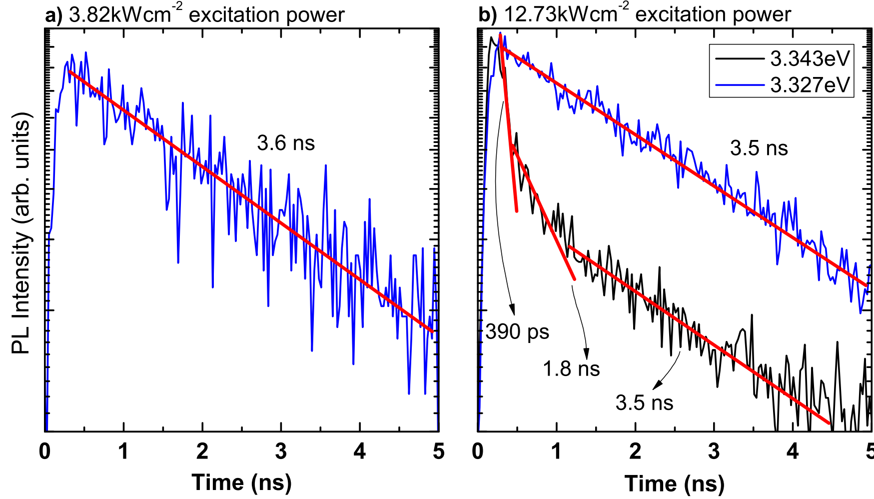

FIG. 7. a) low excitation power (3.82 kWcm^{-2}), and b) high excitation power (12.73 kWcm^{-2}) emission spectra from the nanocolumn as a function of time. Under high excitation power the QDisk emission peak is observed to dynamically return to that which is observed in the low excitation power regime.

TRPL traces at 12.73kWcm^{-2} were measured at wavelength steps of 0.25 nm across the emission peak, and collated into a map showing the luminescence intensity as a function of both emission energy and time (see figure 8). It is clear that the emission dynamically shifts back to that what is observed in the low excitation power regime.

The Blue shift of the QDisk emission with increasing excitation has been observed before, and can be attributed to either fluctuations in the indium content in the QDisk[28], or to charge screening and the quantum confined Stark effect[10,29,30]. The multi-exponential decay at high excitation power, however, is a characteristic feature of a screening of the internal field[31]. In this case, we also note that the measured effect occurs at the same excitation power density range measured by Koukstis *et al.*[28], when they observed the screening of an internal field in

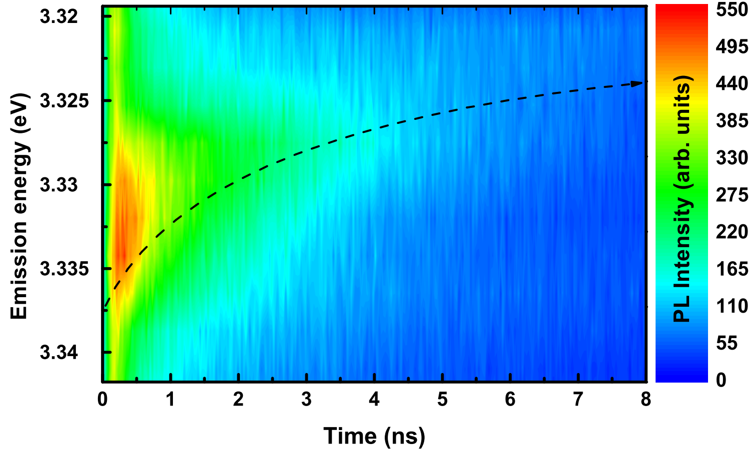

FIG. 8. The luminescence intensity as a function of emission energy and time at an excitation power of 12.73kWcm^{-2}. The emission energy is observed to shift during the process of the decay.

an $In_{0.15}Ga_{0.85}N$ quantum well (at excitation power densities almost two orders of magnitude lower than would be expected for the filling of localized states). Furthermore, as explained above, no measurable blue-shift is observed in QDisk emission with increasing temperature (see figure 5) such that the *maximum* blue shift expected from the filling of these states in this case is 4 meV, 3× smaller than that measured. These observations lead to the conclusion that the effect measured here is mainly due a charge screening process, and that indium content fluctuations play only a minor role, if at all, in the emission shift measured in this case. Local photo-induced heating of the sample is ruled out as a mechanism for the peak energy shift, as the GaN emission is observed at a constant energy for all excitation power densities.

The field screening process is explained as follows: At low excitation powers the carriers in the well are acted on by the internal field such that electrons and holes find themselves at opposite sides of the well. This quantum confined Stark effect results in a lifetime of 3.5 ns, and a lower emission energy. At high excitation powers, however, the large number of carriers at the sides of the well generate their own field to screen the centre of the well from the effects of the internal field. The resulting increased wavefunction overlap leads to a rapid decay (in this case 390 ps) which is an order of magnitude faster than that measured at low excitation powers. This fast emission is at higher energy due to the reduced effect of the internal electric field. As carriers recombine in the disk, the size of the screening field

decreases, and the wavefunction overlap reduces, leading to a dynamic change in both the decay lifetime and the decay energy.

It should be noted, however, that the FWHM of the emission is observed to increase with excitation power, whereas for a screening of the internal field, and hence a reduction in the QCSE we would expect to see a reduction in FWHM with increasing power. The broadening observed here is due to the fact that each spectrum is integrated over a period of 1 second, such that it includes all emission from the energy shift during the process of the decay. FWHM broadening has also been measured by Hou and Tu[32] when they observed field screening in InAsP/InP QWs. It was argued that the broadening is due to interactions between the hot photo-excited carriers, which cannot be ruled out in this case.

The discrepancy can be somewhat alleviated by closer inspection of the data in figure 8. It is possible to probe the time evolution of the emission by recreating the spectrum at various times during the decay (see figure 9). We observe the expected QCSE broadening with increasing time as the screening effect is reduced and the peak is shifted by the increasingly unscreened internal field.

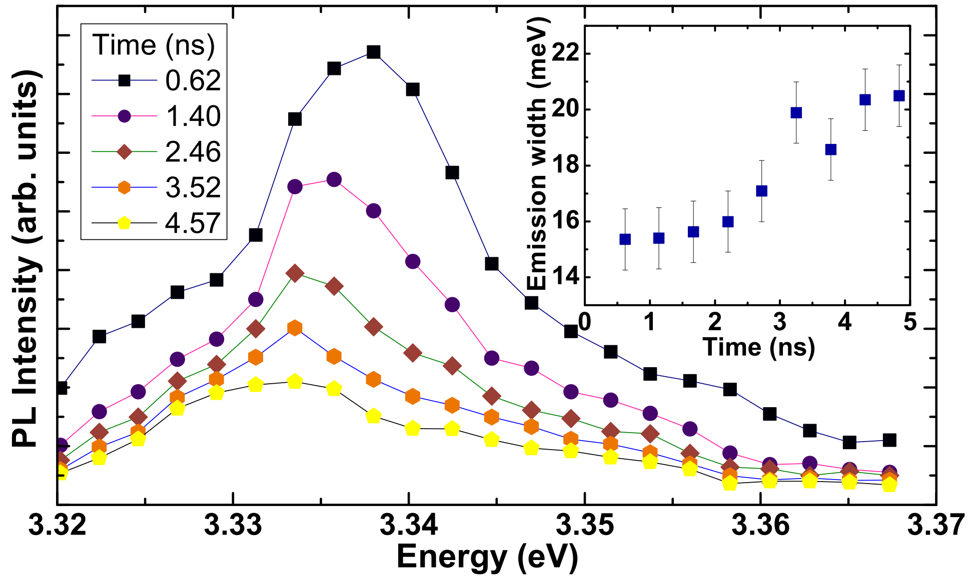

FIG. 9. The decay spectrum at different times (recreated from the data in figure 8). The emission peak broadens as it shifts to lower energy due to the QCSE from the internal field.

C. Further evidence for the QCSE in $In_xGa_{1-x}N$ QDisks

In addition to the data presented above, a study was carried out on several columns containing single QDisks. The low excitation power emission was recorded and the lifetime measured by μ-PL. The data is presented in figures 10(a) and (b). It was found that QDisks emitting at lower energy tend to have longer lifetimes. This can be simply explained by the fact that lower energy emitting QDisks are likely to be slightly thicker, or have a larger indium mole fraction and thus be under more strain. This increased strain would lead to a larger internal electric field which will reduce carrier overlap and enhance the emission lifetime.

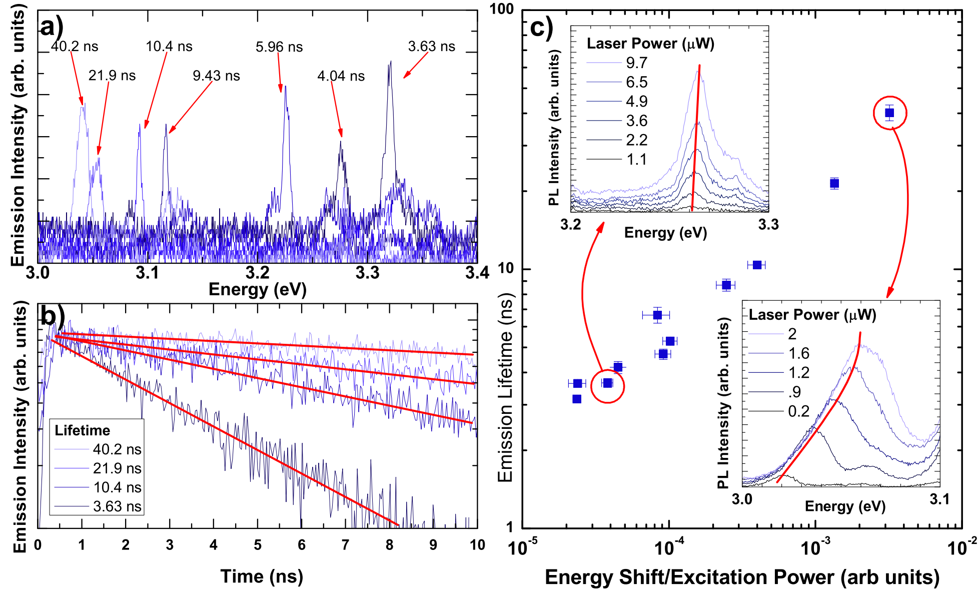

FIG. 10. a) A selection of spectra showing QDisk emissions, labelled with their low power excitation lifetimes. b) a selection of decay traces, showing the monoexponential decay nature of the emission. c) Emission lifetime against the linear gradient of the shift.

Under the influence of the internal electric field, the free carriers move to the top and bottom surfaces of the disk and create a field F which acts to screen the internal field and shift the emission to the blue. The charges at these surfaces will act like a parallel plate capacitor in that the size of the generated field F is proportional to the surface charge density and therefore to the excitation power density. The extent of the shift in emission with increasing excitation power can thus be linked to the dipole moment in the QDisk. The

energy shift under an external electric field F can be modelled[33] as

$$\Delta E = \mu F + \alpha F^2, \tag{1}$$

where μ and α are the projections of the dipole moment, and polarizability onto the direction of F. ΔE is the energy shift caused by the field F.

With this simple model we can estimate the relative projection of the dipole moment along the growth axis for the carriers in the disk by measuring the gradient of the energy shift with increasing excitation power (see figure 10c). We assume that each disk has the same photon absorption probability, and that all disks have the same diameter. It is found that QDisks emitting at lower energies exhibit larger dipole moments. This is what should be expected, as the larger internal fields in the low energy emitting disks should act to give a larger separation of carrier wavefunctions. Indeed, these low energy emitting disks are also the disks with longer lifetimes.

D. Defect emission

In this section we turn our attention to the emission band at 3.40−3.43 eV, which has been rigorously characterised by Calleja *et al.*[9] and has been shown to originate from structural defects in the columns. Our analysis is presented here for completeness and as a comparison to the data presented above, and that in the literature.

Upon close inspection of the defect emission in figure 5, which is now magnified in figure 11a, we observe that the emission consists of multiple narrow peaks. It is found that the minimum width measured from these peaks is 2 meV, and that the relative visibility and peak position vary across the sample, and indeed from sample to sample. The observation of this structure is in agreement with the measurements of Fischer *et al.*[34] who, during their investigation into wurtzite GaN films, observed the emergence of a structure in the emission at 3.41 eV. The structure appears to be more complex in this case however, owing possibly to the measurement technique (μPL as opposed to PL) or perhaps to varying degrees of strain relaxation in neighbouring columns of differing diameter.

A log plot of defect emission spectra with increasing excitation power (The same spectra first presented in figure 7(a)) can be found in figure 11(b). In this case the structure of the emission is not as apparent, and a small shift to higher energy (~ 3 meV) is observed as the

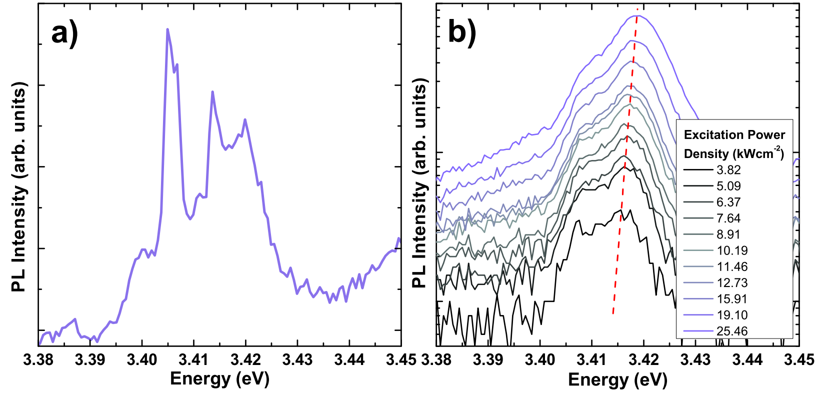

FIG. 11. a) The emission in the region of 3.4 eV to 3.43 eV measured at 4.2 K and with an excitation power of 4.1 kWcm^{-2}. A structure in the emission is clearly visible. b) Log plot of the emission intensity with excitation power from another part of the same sample where the structure is less apparent. A blue shift of the emission with increasing excitation is observed.

excitation power is increased by an order of magnitude from 3.82 to 25.46 kWcm^{-2}. Calle *et al.* measured a similar (~ 5 meV) blue shift for a factor 15 increase in excitation power[35] and attributed it to the saturation of donor-acceptor pairs (DAP). It could be that some of the structure in the broad emission is due structural defects in the column body, and part due to DAP recombination.

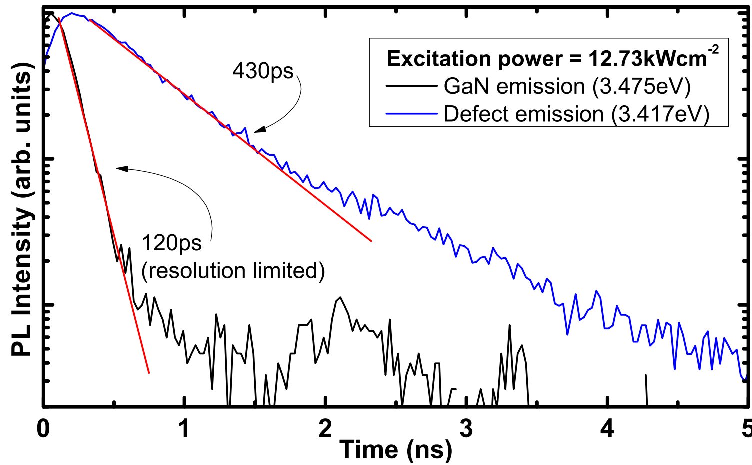

FIG. 12. Normalised time-resolved decays from the GaN emission at 3.475 eV and the defect emission at 3.417 eV measured with an excitation power of 12.73kWcm^{-2}.

A time-resolved decay trace from the defect emission (and also the GaN emission, for comparison) at an excitation power of 12.73 kWcm^{-2} is presented in figure 12. The decay is non exponential, though has a characteristic decay time of 450 ps, in agreement with the study of Calleja *etal.*[9]. Finally (in figure 13) we present a spectrally and time-resolved map of the emission, akin to that of the QDisk emission presented in figure 8. Within the resolution limit of the setup, the defect emission is observed at constant energy during the decay, in contrast to the shifting decay energy of the QDisk emission.

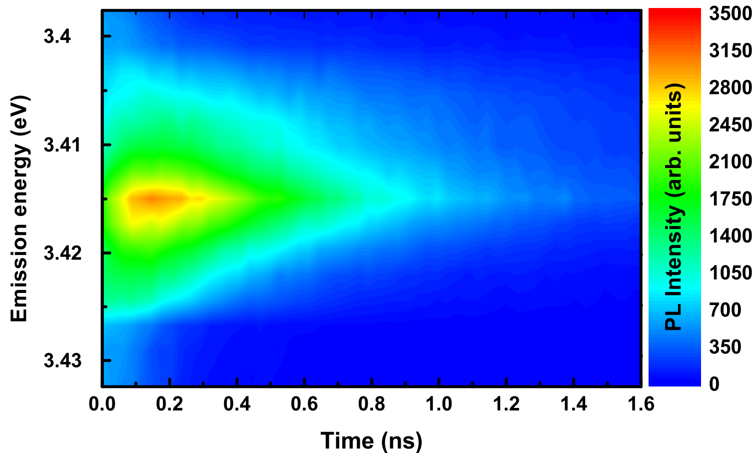

FIG. 13. The luminescence intensity as a function of emission energy and time at an excitation power of 12.73kWcm^{-2}. In contrast to the InGaN QDisk emission, the defect emission does not dynamically shift with time.

VI. SUMMARY

We have carried out μPL investigations on GaN nanocolumns containing low indium content $In_xGa_{1-x}N$ ($x \sim 0.07$) QDisks. The radiative lifetime of the emission at 4 K indicates that there is no lateral charge separation in the QDisks on length scales comparable to the disk radius. It still remains a possibility that carriers are somewhat laterally separated on length scales of a few nm due to localisation at individual localisation centres within the QDisk. The internal electric field results in a separation of carriers in the growth direction. Screening of the internal field has also been observed, characterised by a non-exponential decay, and a lifetime reduction with increasing excitation power.

ACKNOWLEDGMENTS

This research was supported by the Engineering and Physical Sciences Research Council (EPSRC) U.K. (GR/S82176/01). Y S. Park acknowledges funding from the Basic Science Research Program through the National Research Foundation of Korea Grant funded by the Korean Government (2010-0023856).

REFERENCES

[1] S. Nakamura, S. Pearton, and G. Fasol. *The Blue Laser Diode: The Complete Story.* Springer, Berlin, 2000.

[2] F. A. Ponce and D. P. Bour. *Nature (London)*, 386:351, 1997.

[3] W. Shan, W. Walukiewicz, E. E. Haller, B. D. Little, J. J. Song, M. D. McCluskey, N. M. Johnson, Z. C. Feng, M. Schurman, and R. A. Stall. *J. Appl. Phys*, 84:4452, 1998.

[4] M. Laugt, J. Massies, B. Gil, P. Lefebvre, M. Leroux, N. Grandjean, and P. Bigenwald. *Phys. Rev. B*, 58:R13371, 1998.

[5] J. Simon, R. Langer, A. Barski, and N. Pelekanos. *Phys. Rev. B*, (7211), 61.

[6] W. H. Chang, K. U. Tseung, C. M. Lee, C. C. Chuo, C. Y. Lai, T. M. Hsu, and J. I. Chyi. *J. Appl. Phys*, 91:531, 2002.

[7] B. Daudin, G. Feuillet, J. L. Rouviere, N. T. Pelekanos, F. Widmann, and J. Simon. *Phys. Rev. B*, 58:989, 1998.

[8] J. Ristic, C. Riviera, E. Calleja, S. Fernandez-Garrido, M. Povolosyi, and A. Di Carlo. *Phys. Rev. B*, 72:085330, 2005.

[9] E. Calleja, M. A. Sanchez-Garcia, F. J. Sanchez, F. Calle, F. B. Naranjo, E. Munoz, U. Jahn, and K. Ploog. *Phys. Rev. B*, 62:16862, 2000.

[10] Y. Kawakami, S. Suzuki, A. Kaneta, M. Funato, A. Kikuchi, and K. Kishino. *Appl. Phys. Lett.*, 89:163124, 2006.

[11] C. Riviera, U. Jahn, T. Flissikowski, J. L. Pau, E. Munoz, and H. T. Grahn. *Phys. Rev. B*, 75:045316, 2007.

[12] Y. Kawakami, A. Kaneta, L. Su, K. Zhu, M. Funato, A. Kikuchi, and K. Kishino. *J. Appl. Phys*, 107:023522, 2010.

[13]Y. S. Park, S. H. Lee, J. E. Oh, C. M. Park, and T. W. Kang. *J. Cryst. Growth*, 282:313, 2005.

[14]Y. S. Park, C. M. Park, D. J. Fu, T. W. Kang, and J. E. Oh. *Appl. Phys. Lett.*, 85:5718, 2005.

[15]C. M. Park, Y. S. Park, H. Im, and T. W. Kang. *Nanotechnology*, 17:952, 2006.

[16]C. Bocklin, R. G. Veprek, S. Steiger, and B. Witzigmann. *Phys. Rev. B*, 81:155306, 2010.

[17]R. Calarco and M. Marso. *Appl. Phys. A*, 87:499, 2007.

[18]T. D. Veal, P. H. Jefferson, L. F. J. Piper, C. F. McConville, T. B. Joyce, P. R. Chalker, L. Considine, H. Lu, and W. J. Schaff. *Appl. Phys. Lett.*, 89:202110, 2006.

[19]D. M. Graham, A. Soltani-Vala, P. Dawson, M. J. Godfrey, T. M. Smeeton, J. S. Barnard, M. J. Kappers, C. J. Humphreys, and E. J. Thrush. *J. Appl. Phys*, 97:103508, 2005.

[20]E. J. Thrush, M. J. Kappers, P. Dawson, D. Graham, J. S. Barnard, M. E. Vickers, L.Considine, J. T. Mullins, and C. J. Humphreys. *phys. stat. sol. (a)*, 192:354, 2002.

[21]S. F. Chichibu, A. C. Abare, M. P. Mack, M. S. Minsky, T. Deguchi, D. Cohen, P. Kozodoy, S. B. Fleischer, S. Keller, J. S. Speck, J. E. Bowers, E. Hu, U. K. Mishra, L. A. Coldren, S. P. DenBaars, K. Wada, T. Sota, and S. Nakamura. *Mat. Sci. Eng*, B59:298, 1999.

[22]M-Y. Ryu, G. G. Shim, P. W. Yu, E. Oh, Sone Chulsoo, O. Nam, and Y. Park. *Sol. Stat. Comm.*, 120:509, 2001.

[23]X. H. Zhang, W. Liu, and S. J. Chua. *J. Cryst. Growth*, 268:521, 2004.

[24]S. Kalliakos, X. B. Xhang, T. Talierco, P. Lefebvre, B. Gil, N. Grandjean, B. Damilano, and J. Massies. *Appl. Phys. Lett.*, 80:428, 2002.

[25]R. A. Oliver, S. E. Bennet, T. Zhu, M. J. Kappers, D. W. Saxey, A. Cerezo, and C. J. Humphreys. *J. Phys. D*, 43:354003, 2010.

[26]K. Domen, A. Kuramata, and T. Tanahashi. *Appl. Phys. Lett.*, 72:1359, 1998.

[27]M. J. Holmes, Y. S. Park Yand J. H. Warner, and R. A. Taylor. *Appl. Phys. Lett.*, 95:181910, 2009.

[28]E. Kuokstis, J. W. Yang, G. Simin, M. Asif Khan, R. Gaska, and M. S. Shur. *Appl. Phys. Lett.*, 80:977, 2002.

[29]R. Bardoux, A. Kaneta, M. Funato, Y. Kawakami, A. Kikuchi, and K. Kishino. *Phys. Rev. B*, 79:155307, 2009.

[30]Y. S. Park, M. J. Holmes, T. W. Kang, and R. A. Taylor. *Nanotechnology*, 21:115401, 2010.

[31] T. Kuroda and A. Tackeuchi. *J. Appl. Phys*, 92:3071, 2002.

[32] H. Q Hou and C W. Tu. *J. Electon. Mater.*, 25:1019, 1996.

[33] S. A. Empedocles and M. G. Bawendi. *Science*, 278:2114, 1997.

[34] S. Fischer, G. Steude, D. M. Hofmann, F. Kurth, F. Anders, M. Topf, B. K. Meyer, F. Bertram, M. Schmidt, J. Christen, L. Eckey, J. Holst, A. Hoffman, B. Mensching, and B. Rauschenbach. *J. Cryst. Growth*, 189/190:556, 1998.

[35] F. Calle, F. J. Sanchez, J. M. G. Tijero, M. A. Sanchez-Garcia, E. Calleja, and R. Beresford. *Semicond. Sci. Technol.*, 12:1396, 1997.